Applied Scientific Research **48**: 301–314, 1991.
R. V. A. Oliemans (ed.), Computational fluid Dynamics for the Petrochemical Process Industry.

Particle-laden turbulent flows: direct simulation and closure models

S. ELGHOBASHI
Mechanical Engineering Department, University of California, Irvine, CA 92717, USA

Received 25 September 1990; accepted in revised form 15 March 1991

Abstract. This paper presents an overview of the state-of-the-art of direct numerical simulation (DNS) and closure models of particle-laden turbulent flows. The paper also shows how the results of direct simulation can be used to improve current closure models of these flows. Particle dispersion in a decaying grid-turbulence is studied using DNS, and the results are compared with the measurements of Snyder and Lumley (1971).

1. Introduction

Dispersion of solid or liquid particles in turbulent shear flows is of importance in many natural and engineering processes. The transport of pollutants in the atmosphere and oceans, droplets of liquid spray in rocket and internal combustion engines, pulverized coal particles in furnaces, and slurries in pipes are typical examples. At high enough mass loading, the particles modify the turbulence structure in the carrier fluid, hence the modulation of turbulent transport of scalars.

Prediction of these transport phenomena requires knowledge of the two-way nonlinear coupling between the particles and turbulence, i.e. the response of the discrete particles to the turbulent motion of the fluid, and the effect of the particles motion on the frequency spectrum of turbulence. The purpose of this paper is to provide an overview of the state-of-the-art of the numerical approaches of predicting turbulent flows laden with solid particles. It is not intended here to provide a literature review of the subject, rather a review of the methods available at present. It is helpful, before discussing these methods, to classify the regimes of particle-laden turbulent flows from the point of view of the interaction between the particles and turbulence.

Figure 1 shows the different regimes on a diagram using dimensionless coordinates. The quantities appearing on these coordinates are defined below.

Φ_p: volume fraction of particles; $\Phi_p = MV_p/V$; M: number of particles; V_p: volume of particle; V: volume occupied by particles and fluid; S: distance between the centers of two neighboring particles; d: diameter of particle; τ_p: particle response time; τ_K: Kolmogorov time scale; τ_e: turnover time of large eddy.

For very low values of Φ_p ($\leqslant 10^{-6}$) or equivalently large values of S/d ($\geqslant 100$) the particles have negligible effect on turbulence, and the interaction between the particles and turbulence is termed as 'one-way coupling'. This means that particle dispersion, in this first regime, depends on the state of turbulence but there is no feedback to the turbulence.

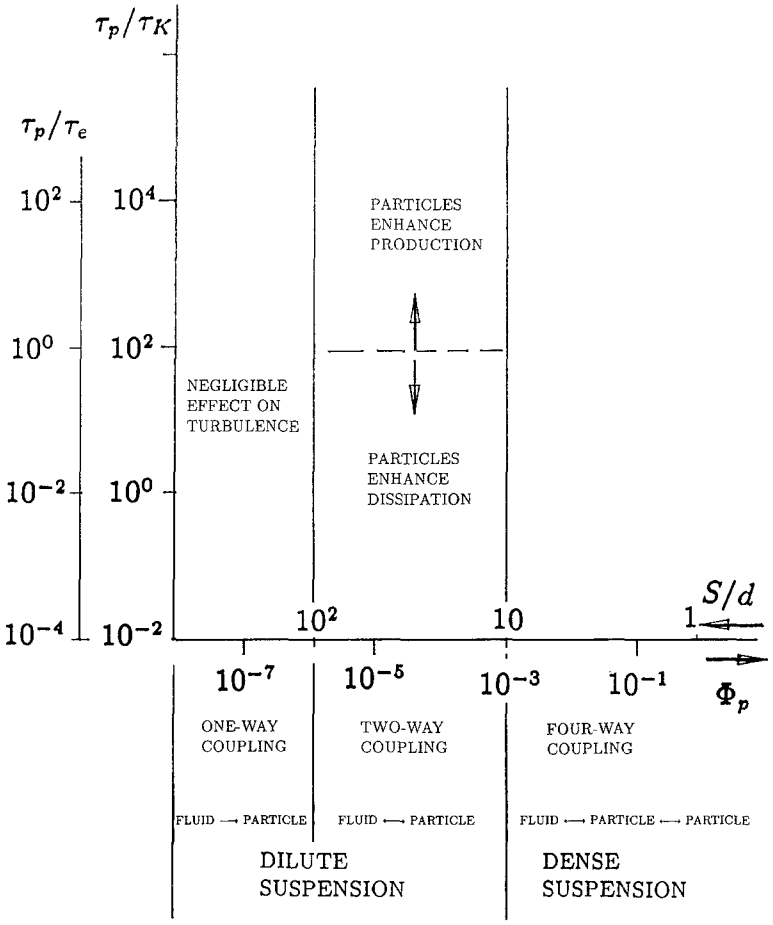

Fig. 1. Map of flow regimes in particle-laden flows.

In the second regime, $10^{-6} < \Phi_p \leqslant 10^{-3}$, $10 \leqslant s/d < 100$, the volumetric particle loading is large enough to alter the turbulence structure, hence the term 'two-way coupling'. Now, in this regime and for a given value of Φ_p, lowering τ_p (e.g. smaller d for the same particle material and fluid viscosity) increases the surface area of the particulate phase, hence the increased dissipation rate of turbulence energy. This is manifested in the modification of the high wave number parts of the spectra of the turbulence energy and dissipation [12]. On the other hand, as τ_p increases for the same Φ_p, the particle Reynolds number, R_p, increases and at values of $R_p \geqslant 400$ vortex shedding takes place resulting in enhanced production of turbulence energy.

Flows in the two regimes discussed above are often referred to as dilute suspensions. In the third regime, because of the increased particle loading, $\Phi_p > 10^{-3}$, $S/d < 10$, flows are referred to as dense suspensions. Here, in addition to the two-way coupling between the particles and turbulence, particle/particle collision takes place, hence the

term four-way coupling. Due to the complexities of flows in this regime, most experimental and numerical studies conducted so far concern dilute suspensions.

The present paper considers only dilute suspensions. First, direct simulation of particle dispersion (one-way coupling) is discussed, and then a summary of turbulence closure models for particle-laden flows is presented.

2. Direct simulation of particle dispersion

In most numerical methods used in predicting particle dispersion in turbulent flows, the instantaneous particle position (trajectory) is calculated from an approximate value of the instantaneous velocity of the fluid surrounding the particle. This velocity is determined from the time-averaged Navier-Stokes equations together with a turbulence closure model and an assumed shape of the velocity pdf. Furthermore, major simplifying assumptions (see Sec. 3) are needed to prescribe the interaction time of a particle with a large-scale turbulence eddy. Some analytical studies assume that the particle resides permanently in an eddy during its lifetime [5]. However, in order to compute particle dispersion accurately it is essential that details of the turbulence structure be computed without the empericism embodied in modeling the time-averaged equations, the assumptions of the pdf shape, or the interaction time between a particle and an eddy.

The method of direct numerical simulation (DNS), on the other hand, provides a modeling-free, three-dimensional, instantaneous velocity field for the fluid in simple turbulent flows. This velocity field can be used to calculate the three-dimensional trajectory of a particle from which the dispersion statistics can be obtained. This is the approach adopted in the work to be presented here. This work is part of a study of particle dispersion [11], [10], and turbulence modulation [12] in unsheared and sheared turbulence. The following summarizes other published DNS studies of particle dispersion.

Riley and Patterson [21] were the first to present a computer simulation of the Lagrangian statistics of a solid particle in a numerically integrated, decaying isotropic turbulence. The fluid Eulerian velocity field was obtained by direct numerical simulation of turbulence in a cubical volume (32^3 grid points), with an initial microscale Reynolds number $R_\lambda = 23$. The particle trajectory was obtained from the numerical solution of the equation of particle motion including only the Stokes drag. As expected, their simulation showed that increasing the response time of the particle increased its velocity autocorrelation coefficient, a result contradictory to experimental observation (Snyder and Lumley [22]). This discrepancy is due to the absence of the gravity term from the particle motion equation, eliminating the effects of crossing trajectories (Yudine [27]).

Squires and Eaton [23] studied the effect of particles on stationary isotropic turbulence. The stationarity was achieved by artificially forcing the low wave number modes. The simulation used 32^3 grid points. The particle equation included only the

Stokes drag force. The simulation showed that increasing the mass loading lowers the turbulence energy of the carrier fluid.

McLaughlin [18] computed particle trajectories in a numerically simulated vertical channel flow, with $16 \times 64 \times 65$ grid points, to study particle deposition on the wall. The equation of motion of the particle included the Stokes drag and Saffman lift force, but not the gravity, virtual mass, and Basset history terms. It was found that although the magnitude of Saffman lift force was less than that of the component of Stokes drag normal to the wall, the impulse provided by the lift force had a significant effect on particle deposition within the viscous sublayer. The reason is that in this region the normal component of fluid velocity is relatively small. The Saffman lift force tends to trap the particles within the viscous sublayer.

2.1. *Computation of particle trajectories*

The instantaneous velocity, v_i, in the x_i direction, of each particle is obtained by time integration of the following Lagrangian equation of particle motion:

$$\begin{aligned} m_p(\mathrm{d}v_i/\mathrm{d}t_p) = {} & m_p F(u_i - v_i) + m_f(Du_i/Dt) \\ & + \tfrac{1}{2} m_f(Du_i/Dt - \mathrm{d}v_i/\mathrm{d}t_p) \\ & + 6a^2(\pi\rho\mu)^{1/2} \int_{t_{p_0}}^{t_p} \frac{\mathrm{d}/\mathrm{d}\tau(u_i - v_i)}{(t_p - \tau)^{1/2}}\,\mathrm{d}\tau \\ & + (m_p - m_f)g_i \end{aligned} \tag{1}$$

Equation 1 describes the balance of forces acting on the particle as it moves along its trajectory. The term on the left hand side is the inertia force acting on the particle due to its acceleration. The terms on the right side are respectively the forces due to viscous and pressure drag, fluid pressure gradient and viscous stresses, inertia of virtual mass, viscous drag due to unsteady relative acceleration (Basset), and buoyancy. F if the inverse response time of the particle. The response time is the time for momentum transfer due to drag. F is calculated from:

$$F = 1/\tau_p = \left(\frac{3}{8a}\right) C_D \left(\frac{\rho}{\rho_p}\right) |u_i - v_i|. \tag{2}$$

The quantities a, m_p, ρ_p are respectively the particle radius, mass and material density. C_D is the drag coefficient, which is assumed a function of the Reynolds number of the particle, $R_p = 2a\rho|u_i - v_i|/\mu$. The fluid density and viscosity are ρ and μ. $\mathrm{d}/\mathrm{d}t_p$ is the derivative with respect to time following the moving particle, whereas Du_i/Dt is the total acceleration of the fluid as seen by the particle,

$$\frac{Du_i}{Dt} = \left[\frac{\partial u_i}{\partial t} + u_j \frac{\partial u_i}{\partial x_j}\right],$$

evaluated at the particle position $\mathbf{x}_p$. Both u_i and v_i are measured with respect to a coordinate system that is moving with a constant mean stream velocity in the vertical (x_3) direction, i.e. opposite to that of the gravitational acceleration. This simple transformation removes the effects of mean advection and allows us to examine the influence of turbulent fluctuations on solid and fluid particle dispersion which is of main interest here.

Equation 1 has a long history dating back to Stokes [24], followed by Basset [2], Boussinesq [4] and Oseen [19]. It has undergone extensive modifications starting with Tchen [26], followed by Corrsin and Lumley [6], Lumley [15], Maxey and Riley [17] and Auton [1] among others. It is well known that Eq. 1 has no exact solution, except for a trivial case, even in its simplest form in which all but the first term on the r.h.s. vanishes. This is due to the nonlinearity originating from the need to evaluate the fluid velocity, u_i, at the yet unknown particle position.

It should be noted that if the particle Reynolds number R_p is not small, permitting a Stokes approximation, no exact explicit equation of motion is known [16]. Of course the flow around the particle is determined by the Navier-Stokes equations, but the resulting drag is not a simple function of the relative velocity.

The integration of Eq. 1, via a second order Adams-Bashforth scheme provides the new velocity, $v_i(t)$, in the x_i direction for each particle as a function of time. The new position, $x_{p,i}(t_n)$ is calculated from:

$$x_{p,i}(t_n) = x_{p,i}(t_{n-1}) + \Delta t[v_i(t_n) + v_i(t_{n-1})]/2, \tag{3}$$

where t_{n-1} is the time at the previous time-step, and $\Delta t = t_n - t_{n-1}$.

The fluid velocity $u_i[x_{p,i}(t)]$ at the particle location (initially, the coincident fluid and particle velocities are assumed equal), which is needed to integrate Eq. 1 is obtained by a fourth-order accurate, two-dimensional, four-point Hermitian cubic polynomial interpolation scheme between the adjacent Eulerian fluid velocity values. This scheme is applied in the three coordinate directions at the particle location.

Initially, a number of particles, e.g. 16^3, is uniformly distributed within the computational box where there are 64^3 grid points. The initial velocity of each particle is assumed equal to the fluid velocity at the same location. Eq. 1 is then integrated, for a given time-step Δt, in the three coordinate directions to obtain the subsequent particle velocity, and calculate the new position from Eq. 3.

2.2. Simulation of grid-generated turbulence

The exact time-dependent, three-dimensional continuity and Navier-Stokes equations under periodic boundary conditions are integrated in a cubical domain with side length L; $L = 1$. The domain moves with the constant mean stream velocity in the vertical positive x_3 direction, thus the dependent variables of the four governing equations are the instantaneous fluctuations of the three velocity components, u_i, and the pressure. The fluid is incompressible and has a constant kinematic viscosity, ν.

The equations are discretized in an Eulerian framework using a second-order finite-difference technique on a staggered grid containing N^3 points. N is an even number of points which are equispaced within the length L in each of three coordinate directions. The Adams-Bashforth scheme is used to integrate the equations in time. Pressure is treated implicitly, and is obtained by solving the Poisson equation in finite-difference form using a fast Poisson solver. More details about the numerical method are discussed in [13] and [10].

The initialization algorithm insures, for a prescribed energy spectrum, that the initial random velocity field is isotropic, periodic in the three spatial directions, and divergence-free with respect to the discretized form of the continuity equation.

2.3. *Results*

The results presented here are for two particles (corn pollen and copper) selected from the four used by Snyder and Lumley [22]. The diameter and density, hence τ_p, of the two particles used in the simulation are identical to those in the experiment of Snyder and Lumley, referred to hereinafter as SL. The values of d, ρ_p, τ_p of the corn particle are respectively 87μ, $1000\,\mathrm{kg/m^3}$, and $0.02\,\mathrm{sec}$ and those for the copper particle are 46.5μ, $8900\,\mathrm{kg/m^3}$, and $0.049\,\mathrm{sec}$. The dispersion statistics include the mean-square displacement, turbulent diffusivity, and the time development of the forces acting on the solid particle. Only a sample of the results is presented here. The complete set of results and a comprehensive discussion of the physics of particle dispersion are published elsewhere [10].

The mean-square displacement (dispersion) of a solid or fluid particle in the x_i direction is calculated from:

$$\langle x_{p,i}^2(t)\rangle = (1/N)\sum_{j=1}^{N}[x_{p,i}(t) - x_{p,i}(t_0)]_j^2, \tag{4}$$

where N is the total number of particles and t_o is the starting time of calculating the statistics. Figure 2 shows the time development of the lateral $\langle x_{p,2}^2(t)\rangle$ of the two particles, normalized by l_o^2, where l_o is the initial integral length scale. As expected, the lighter particle (corn) with smaller τ_p disperses laterally more than the heavier copper particle. The agreement is acceptable for the copper particle throughout the entire range of SL's data. Better agreement has been obtained for the simulations with higher resolution [10]. The corn particle displacements in the simulation are initially lower than in the experiment but the agreement improves monotonically with time as we approach the long-time dispersion regime.

Also shown in the figure are the time development of $\langle x_{p,2}^2\rangle$ of a corn particle in zero gravity and of the corresponding fluid point. The effect of gravity in reducing particle dispersion in the lateral direction is evident in the figure. It is also seen that in zero-gravity, the corn particle disperses in the lateral direction slightly more than the corresponding fluid point.

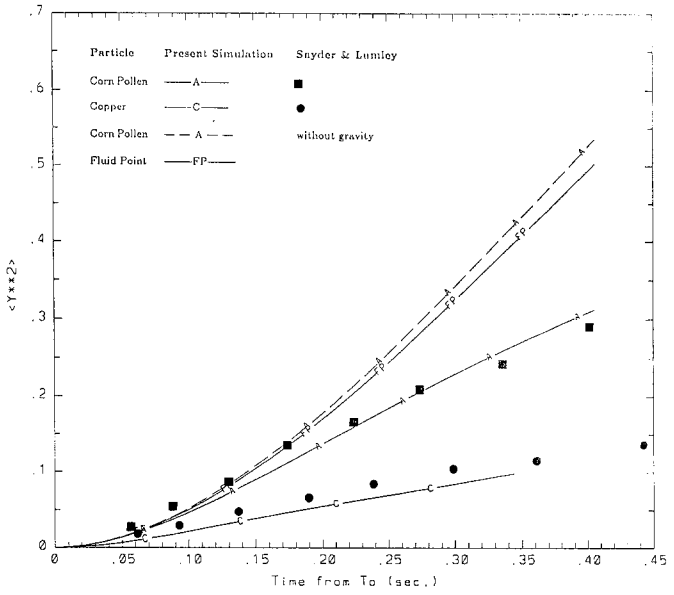

Fig. 2. Normalized mean-square displacement in the lateral direction (y).

In the absence of gravity, the solid particle stays longer in an eddy before it crosses to another. However, due to its finite inertia, the particle continues along its trajectory with little change in its velocity. The fluid point, on the other hand, responds instantaneously to the local dynamics of turbulence (e.g. vortex stretching and the associated pressure fluctuations and enstrophy) and thus its velocity changes in magnitude and direction at a rate faster than that of the particle, hence a smaller velocity autocorrelation than that of the particle.

It can be shown (Batchelor [3]) that the turbulent diffusivity of a fluid point, $D_{fp,i}$, in a homogeneous turbulence is related to its mean-square displacement via

$$D_{fp,i}(t) = \frac{1}{2}\frac{\mathrm{d}}{\mathrm{d}t}\langle x_{fp,i}^2(t)\rangle. \tag{5}$$

Based on the results of Taylor's theory [25], it is expected that the diffusivities $D_{p,i}$ and $D_{fp,i}$ of the solid particle in zero gravity and its corresponding fluid point vary linearly with time, after short dispersion times, and be independent of time for long times. Figure 3, which shows the time development of $D_{p,i}$ and $D_{fp,i}$ for the corn particle in zero gravity, supports this conclusion. Again, as was shown in Fig. 2, the solid particle in zero gravity, due to its finite inertia, disperses laterally faster than their corresponding fluid points. Also shown are the numerical and experimental $D_{p,i}(t)$ for the copper particle. The agreement between the numerical and experimental values of $D_{p,i}(t)$ is reasonable.

Figure 4 shows the time development of the relative velocity and the forces acting

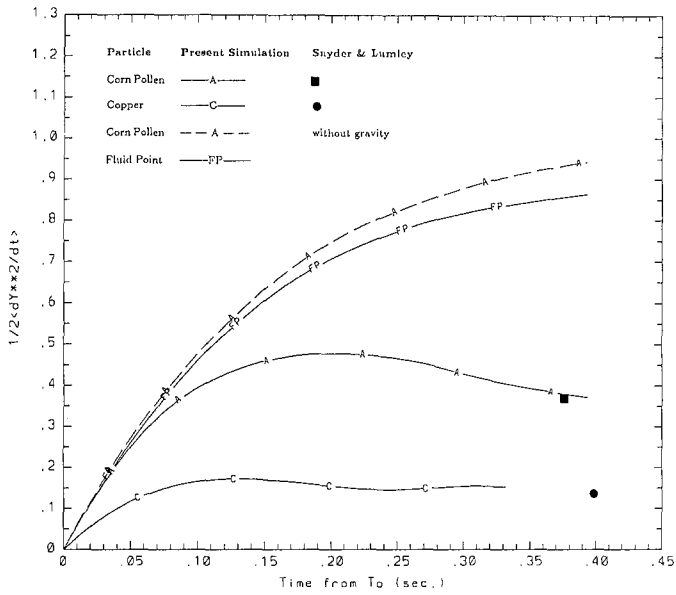

Fig. 3. Normalized turbulent diffusivities in the lateral direction (y).

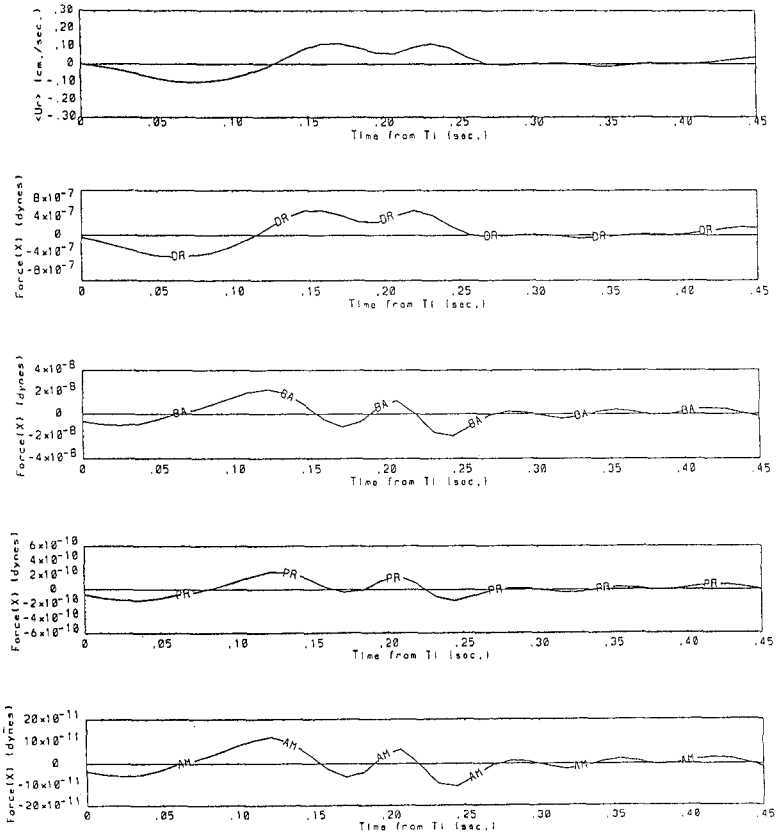

Fig. 4. Forces (in dynes) on the copper particle in the lateral direction (x). DR: Drag, BA: Basset, PR: Fluid pressure gradient, AM: Added mass.

on the copper particle starting from the time of its injection into the decaying grid turbulence in gravity environment. The x_1-component of the drag and Basset forces, and those due to pressure gradient and added mass are presented first without normalizing (in dynes). It is seen that the amplitudes of the fluctuations of the relative velocities and forces diminish with time indicating that the particles are asymptotically approaching velocity equilibrium with the decaying turbulence. Figure 5 shows the forces normalized by the drag to examine their relative significance. It can be concluded from Figs. 4 and 5 that in isotropic decaying turbulence that the drag is the main force controlling the particle motion in the lateral directions, i.e. in the plane normal to gravity. It is also seen that the Basset force, though one order of magnitude smaller than the drag, is orders of magnitude larger than the other two forces, and thus may become important in other flow situations where flow reversal or sudden acceleration/deceleration takes place.

In the gravity direction, the time development of the forces [10] indicates that drag and gravity forces are of equal significance in controlling the particle dispersion in that direction.

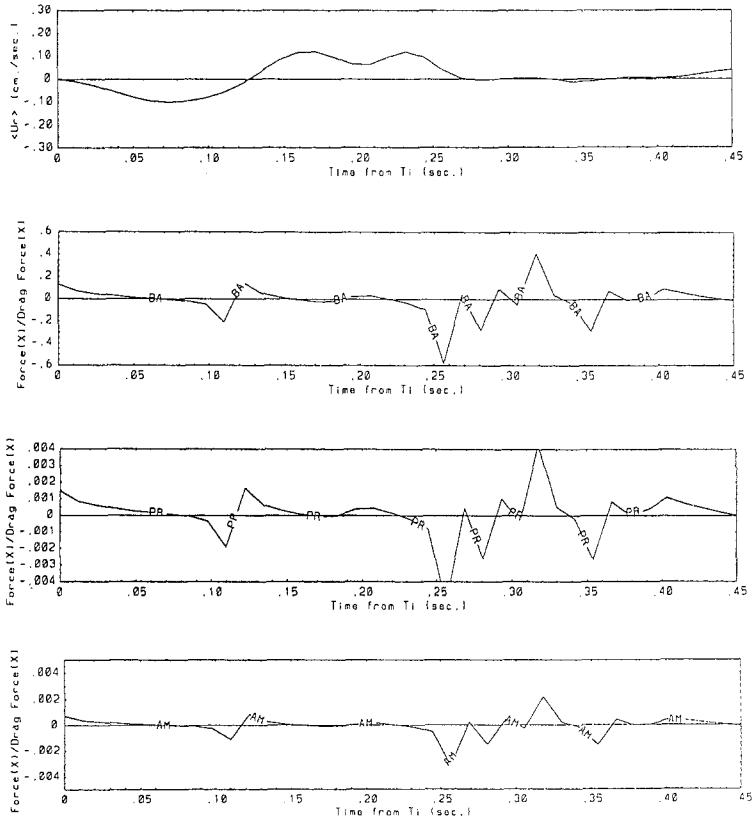

Fig. 5. Forces on the copper particle in the lateral direction (x) normalized by the drag force. BA: Basset/Drag, PR: Fluid pressure gradient/Drag, AM: Added mass/Drag.

3. Closure models for particle-laden flows

Table 1 below compares the two approaches used currently in predicting particle-laden flows, namely the Eulerian (or two-fluid) and the Lagrangian (or particle trajectory). The main difference between the two approaches lies in the treatment of the dispersed phase.

In the two-fluid method, the particulate phase is considered, under certain assumptions [8], as a continuum, and thus its velocity field is determined from the solution of its time-averaged, volume-averaged Navier-Stokes equations. The interaction between the two phases is accounted for in their respective Navier-Stokes equations via the drag and buoyancy forces. Turbulent diffusion (dispersion) of the particulate phase is calculated by modeling the turbulent fluxes such as $\langle \phi_2 v_i \rangle$.

In the Lagrangian method, the trajectories of the individual particles are computed from Eq. 1 and Eq. 3. However, the instantaneous velocity of the surrounding fluid $u_i(t)$ needed in these two equations is approximated from the kinetic energy of turbulence, together with an assumed pdf of $u_i(t)$ and the residence time of a solid particle in a turbulence eddy. Typically, it is assumed [14] that the turbulence is isotropic and the pdf of the velocity fluctuation is Gaussian despite the inhomogeneity of the flow. This assumption allows the velocity fluctuation to be calculated from the local value of the turbulence kinetic energy. The local instantaneous velocity is then obtained by simply adding the velocity fluctuation to the mean velocity in a given direction from the time-averaged Navier-Stokes equations. Now further assumptions are needed to calculate the time during which the particle is surrounded by a fluid

Table 1. Current closure models for particle-laden flows

Eulerian (two-fluid)	Lagrangian (Particle Trajectory)
Mean motion	
Time-averaged momentum eqs. *for each phase.*	Time-averaged momentum eq. for the *fluid phase* only
$k - \varepsilon$ equations for the fluid	$k - \varepsilon$ equations for the fluid.
Dispersion	
Model terms like $\langle \phi_2 v_i \rangle$ in continuity, and $\langle \phi_2 p_{,i} \rangle$ in momentum If gradient transport is used, then ν_ϕ is modelled as ν_t/σ_ϕ, where σ_ϕ is a semi-empirical input	Particle trajectory is obtained from solution of particle equation. The instantaneous velocity of fluid surrounding the particle is obtained from k, assuming: (a) the shape of the local pdf of $u_i(t)$, and (b) the size of zone of fluid-particle interaction, or residence time of a particle in an eddy.
Turbulence modulation	
Model correlations appearing in $k - \varepsilon$ equations, e.g. $F\Phi_2 \langle u_i(v_i - u_i) \rangle$ which represents extra dissipation, and $U_k \langle u_i(\phi_1 u_i)_{,k} \rangle$, which represents extra production.	Add source/sink terms in $k - \varepsilon$ equations, corresponding to the source terms in the momentum equation, and the number of particles residing in an eddy.

having that instantaneous velocity. Usually [14] it is assumed that this interaction time equals the smaller of the eddy turnover time and the time it takes a particle to cross an eddy along a straight line.

A slightly different approach [7] in estimating the instantaneous velocity of the fluid surrounding the discrete particle is to follow simultaneously the trajectories the particle and a fluid point by solving their respective Lagrangian equations of motion. The assumption of Gaussian pdf if also invoked here to obtain the instantaneous fluid velocity from the time-averaged momentum equations. The instantaneous velocity of the fluid surrounding the particle is obtained from the Eulerian velocity correlation within a domain centered around the fluid point and whose size equals the eddy size.

When the volume fraction of the particles is large enough, i.e. in the two-way coupling regime of Fig. 1, the effect of particles on turbulence is obtained by modeling the correlations, in the kinetic energy and dissipation equations of the fluid, containing the volume fraction of the particulate phase as shown in Table 1.

In flows where the volume fraction of the particles is vanishingly small then we have, as shown in Fig. 1, a one-way coupling regime in which the particles have negligible effect on the turbulence. Accordingly, the transport equations of the turbulence energy and dissipation rate become identical to those of the single-phase flow. In other words, these equations would not contain any correlations involving the dispersed phase. The reason is that these equations are derived from the Navier-Stokes equations of the fluid using both time-averaging and volume-averaging. When the number of particles per unit volume is vanishingly small then the continuum assumption for the dispersed phase becomes invalid, and any correlation involving the *particulate phase* would be meaningless. In that case, particle dispersion statistics can be studied only via the Lagrangian approach.

In addition to the two approaches described above, Reeks [20] recently introduced a new method for dilute suspensions based on the ideas of the kinetic theory of gases. First, a transport equation is derived for the average phase space density of particles of velocity v at position x and time t. This equation, which is analogous to Boltzmann equation, is then used to derive the balance equations of mass, momentum and energy of the dispersed phase. However, as expected, the momentum and energy equations are unclosed, and thus require constitutive relations for the pressure tensor and kinetic energy flux. Reeks [20] indicated that an examination of the pressure tensor for a particle-laden uniform shear flow revealed that the dispersed phase does not behave as a simple fluid.

3.1. Validation of closure models using results of direct simulation

In the process of developing a two-equation turbulence model for particle-laden flows, Elghobashi and Abou Arab [8] derived the exact transport equations for the fluid turbulence kinetic energy and its dissipation rate which account for the presence of the dispersed particulate phase. One of the important terms in the energy equation which

represents the additional dissipation of energy due to the particles is:

$$F\Phi_2\overline{u_i(v_i - u_i)}$$

where Φ_2 is the local volume fraction of the particles, F is the inverse response time of the particle defined in Eq. 2, and (u_i, v_i) are the local instantaneous velocities of the fluid and particles respectively in the $i-$ direction.

In order to evaluate the correlations $\overline{u_i(v_i - u_i)}$, Elghobashi and Abou Arab [8] used Chao's solution [5] of the linearized equation of particle motion and proposed the following model:

$$\overline{u_i(v_i - u_i)} = -(1/2)\overline{u_i^2}\left[1 - \int_0^\infty \frac{\Omega_1 - \Omega_R}{\Omega_2} f(\omega)\,\mathrm{d}\omega\right], \tag{6}$$

where Ω_1, Ω_2 and Ω_R are functions of the turbulence frequency, ω, fluid density and viscosity, particle density and particle diameter. The exact forms of these functions are given in [8].

Now the validity of the model presented in Eq. 6 has been examined only indirectly by comparing the predicted time-averaged correlations, like the turbulent stresses, with their measured values in a turbulent particle-laden jet by Elghobashi et al. [9]. What is needed is a direct evaluation of the term on the right hand side of eq. 6 by using the results of the direct simulation. This will provide validation of the model described by eq. 6. If the model proves inadequate then it can be improved so as to agree with the results of the direct simulations. Models of the other terms in the energy and dissipation equations can also be evaluated.

The above discussion provides an example of how the results of DNS can be used to validate and improve existing closure models for particle-laden flows. There are other models for particle diffusivities and autocorrelations that require close examination, especially that almost all of them are based on the assumption of small particle Reynolds number (≈ 1) to justify the use of Stokes drag.

4. Closing remarks

(1) DNS provides detailed information, unavailable otherwise, about particle dispersion and effects of particles on turbulence. This information can be used to improve current closure models or develop more realistic models.
(2) Closure models for particle-laden flows (Eulerian or Lagrangian) are needed at present and in the foreseeable future for complex geometries in industrial applications, since the power limitations of current supercomputers do not permit the application of DNS to complex turbulent flows.
(3) Large eddy simulation (LES) combined with the Lagrangian equation of particle motion (especially for $d \gg \eta$) shows promise in simple geometries (channel).

(4) More work (coordinated experimental, numerical and theoretical) is needed to extend the domain of validity of the equation of single particle motion to high values of R_p in turbulent shear flows.

Some of the questions to be answered are:

(a) What is the effect of turbulence in the surrounding fluid on the drag, lift, Basset force?

(b) In dilute suspension, what are the effects of the wakes of the neighboring particles on the forces in the equation of motion of a single particle?

(c) In dense suspension, how to account for the particle-particle collision in the equation of motion of a single particle?

Acknowledgements

The computations presented in this paper have been performed on the supercomputers Cray XMP/48, Cray YMP and Cray 2 at two computer centers whose support is acknowledged. These centers are the San Diego Supercomputer Center (SDSC) and the Numerical Aerodynamic Simulation (NAS) at NASA-Ames. This work was also supported in part by the University of California, Irvine, through an allocation of computer time on the Convex-C240 supercomputer. The contents of this paper were presented in an invited lecture at the Shell Conference on Computational Fluid Dynamics, Apeldoorn, The Netherlands, December 1989. The author acknowledges the financial support and hospitality of Shell during the stay in Apeldoorn.

References

1. Auton, T. R. The dynamics of bubbles, drops and particles in motion in liquids. *Ph.D. Thesis*, Cambridge University (1983).
2. Basset, A. B.: *A treatise on hydrodynamics*. Dover, N.Y. 2 (1988) 285.
3. Batchelor, G.K.: Diffusion in a field of homogeneous turbulence. *Aust. J. Sci. Res.* A2 (1949) 437–450.
4. Boussinesq, J.: Theorie analytique de la chaleur. Paris 2 (1903) 224.
5. Chao, B. T.: Turbulent transport behavior of small particles in dilute suspension. *Osterr. Ing. Arch.* 18 (1964) 7.
6. Corrsin, S. and Lumley, J. L.: On the equation of motion for a particle in turbulent fluid. *Appl. Sci. Res.* 6 (1956) 114–116.
7. Desjonqueres, P., Berlemont, A. and Gouesbet, G.: Lagrangian simulation of turbulence modification in three particle-laden turbulent round jets. *Third Joint ASCE/ASME Mechanics Conference*, Univ. Calif., San Diego (1989) 7–12.
8. Elghobashi, S. E. and Abou Arab, T. W.: A two-equation turbulence model for two-phase flows. *Phys. Fluids* 26 (1983) 931.
9. Elghobashi, S. E., Abou Arab, T. W., Rizk, M. and Mostafa, A.: Prediction of the particle-laden jet with a two-equation turbulence model. *Int. J. Multiphase Flow* 10 (1984) 697.
10. Elghobashi, S. E. and Truesdell, G. C.: Direct simulation of particle dispersion in decaying isotropic turbulence. *J. Fluid Mech.*, submitted, July, 1990.
11. Elghobashi, S. E. and Truesdell, G. C.: Direct simulation of particle dispersion in grid turbulence and homogeneous shear flows. *Bull. Am. Phys. Soc.* 34 (1989) 2311.

12. Elghobashi, S. E. and Truesdell, G. C.: On the interaction between solid particles and decaying turbulence. *Eighth Symposium on Turbulent Shear flows*, submitted, November, 1990.
13. Gerz, T., Schumann, U. and Elghobashi, S.: Direct simulation of stably stratified homogeneous turbulent shear flows. *J. Fluid Mech.* 200 (1989) 563–594.
14. Gosman, A. D. and Ioanides, E.: Aspects of computer simulation of liquid-fuelled combustors. *AIAA 19th Aerospace Sciences Meeting, St. Louis, MO*, Paper no. 81-0323 (1981).
15. Lumley, J. L.: Some problems connected with the motion of small particles in a turbulent fluid. *Ph.D. Thesis*, Johns Hopkins University 41 (1957).
16. Lumley, J. L.: Two-phase and non-newtonian flows. *Topics in Physics* 12 (1978) 290–324.
17. Maxey, M. R. and Riley, J. J.: Equation of motion for a small rigid sphere in a nonuniform flow. *Phys. Fluids* 26 (1983) 883–889.
18. McLaughlin, J. B.: Aerosol particle deposition in numerically simulated channel flow. *Phys. Fluids* A1 (1989) 1211–1224.
19. Oseen, C. W.: Uber die stokes'sche formel, und uber eine verwandte aufgabe in der hydrodynamik. *Hydromechanik*, Leipzig, 82 (1927) 82.
20. Reeks, M. W.: On the momentum and energy equations for a dispersed particle flow. *Third Joint ASCE/ASME Mechanics Conference*, Univ. Calif., San Diego (1989) 13–14.
21. Riley, J. J. and Patterson, G. S. Jr.: Diffusion experiments with numerically integrated isotropic turbulence. *Phys. Fluids* 17 (1974) 292.
22. Snyder, W. H. and Lumley, J. L.: Some measurements of particle velocity autocorrelation functions in a turbulent flow. *J. Fluid Mech.* 48 (1971) 41.
23. Squires, K. D. and Eaton, J. K.: Study of the effects of particle loading on homogeneous turbulence using direct numerical simulation. *Third Joint ASCE/ASME Mechanics Conference*, Univ. Calif., San Diego (1989) 37–44.
24. Stokes, G. C.: On the effect of the internal friction of fluids on the motion of pendulums. *Trans. Camb. Phil. Soc.* 9 (1851) 8.
25. Taylor, G. I.: Diffusion by continuous movement. *Proc. Lond. Math. Soc.* A20 (1921) 196.
26. Tchen, C. M.: Mean value and correlation problems connected with the motion of small particles suspended in a turbulent fluid. *Ph.D. Thesis*, Delft University, Martinus Nijhoff, The Hague (1947).
27. Yudine, M. I.: Physical considerations on heavy-particle diffusion. *Adv. Geophys.* 6 (1959) 185–191.